

^{119}Sn Mössbauer-effect studies in Heusler alloys $\text{Pd}_{1+z}\text{MnSb}_{1-x}\text{Sn}_x$ — Compositional and heat-treatment effects

M. Tenhover* and P. Boolchand

Department of Physics, University of Cincinnati, Cincinnati, Ohio 45221

(Received 23 January 1978)

Mössbauer-effect experiments on samples of $\text{Pd}_2\text{MnSb}_{0.99}\text{Sn}_{0.01}$ performed systematically as a function of heat treatment have revealed the existence of three ^{119}Sn magnetic field sites characterized by high-, intermediate-, and low-field values. A high-field site of 210 ± 5 kOe is identified with Sn replacing Sb in the ordered $L2_1$ structure of Pd_2MnSb . An intermediate-field site of about 100 kOe is identified with a defect Sn environment which probably consists of 4 Pd vacancies in the near-neighbor coordination of the regular high-field site. The identification of the intermediate-field site is suggested by a set of measurements performed as a function of Pd composition z in $\text{Pd}_{1+z}\text{MnSb}_{0.995}\text{Sn}_{0.005}$ samples, which revealed the Sn field in the $C1_b$ structure of PdMnSb to be 100 kOe. Finally, a low-field site (~ 0 kOe) is observed on prolonged annealing $\text{Pd}_2\text{MnSb}_{0.99}\text{Sn}_{0.01}$ samples. This site is shown to be formed irreversibly due to the presence of oxygen contamination and represents a defect Sn site whose structure is less certain. The ^{119}Sn field results in PdMnSb and Pd_2MnSb hosts are compared with estimates of these fields based on the Jena-Geldart model.

I. INTRODUCTION

Although internal magnetic fields in Heusler alloys $X_2\text{MnY}$ have been measured for over a decade, it is clear that our present understanding of these data is far from complete. Attempts to gain a fundamental understanding of the origin of fields in these ternaries have come recently through the systematics of fields at $5sp$ impurities substituted at the Sb site in the well-characterized Heusler alloys Pd_2MnSb and PdMnSb . A number of recent publications dwelling on the experimental¹⁻⁸ and theoretical^{9,10} aspects of this problem have appeared and these seem to reinforce the expediency in pursuing this approach. Unfortunately, in some of these measurements, from an experimental point of view, important questions concerning the metallurgy of the $5sp$ impurity in question with the Heusler alloy host have not been clarified, leading to serious discrepancies in field measurements. The case of the impurity Sn in Pd_2MnSb appears to be one such example.

A clearly resolved Sn magnetic hyperfine structure in ferromagnetic Pd_2MnSb was first observed by us³ and more recently by others,⁵ suggesting a Sn field value of $+210 \pm 5$ kOe at 4.2 K in the indicated Heusler alloy. Previous study of the ^{119}Sn hyperfine interaction in Pd_2MnSb was also reported by Campbell and Leiper,⁸ who observed a much smaller field of about 10 kOe. The large discrepancy between these field results has remained unexplained. In this paper, we show the existence of thermally induced structural and metallurgical effects in the Sn-doped Pd_2MnSb samples. Induction melted samples of $\text{Pd}_2\text{MnSb}_{0.99}\text{Sn}_{0.01}$

used as absorbers in these ^{119}Sn Mössbauer-effect (ME) experiments exhibit three distinct hyperfine field sites. The population of these sites is found to be sensitive to the heat treatment undergone by the alloy. In the present paper, we attempt to elucidate these heat treatment effects and to identify the magnetically inequivalent sites.

Of the few available $5sp$ Mössbauer-effect probes that can be utilized to investigate Heusler alloys, ^{119}Sn is in a sense unique. One can pursue room-temperature measurements in this spectroscopy and thus investigate the paramagnetic phase of Pd_2MnSb . Systematic changes in room-temperature isomer shift (IS) of $\text{Pd}_2\text{MnSb}_{0.99}\text{Sn}_{0.01}$ samples were observed as a function of thermal history undergone by the samples. A correlation of these IS's with the internal fields is made to elucidate the observed annealing effects in this system.

Two other types of experiments were also undertaken in this work. Measurements were performed as a function of Pd composition z in $\text{Pd}_{1+z}\text{MnSb}_{0.995}\text{Sn}_{0.005}$ samples with the purpose of measuring the Sn field in the $C1_b$ structure of PdMnSb . Secondly, the compositional behavior of the Sn field in the $\text{Pd}_2\text{MnSb}_{1-x}\text{Sn}_x$ system was systematically studied. We show in this paper that these data reveal a smooth composition behavior, which is suggestive of miscibility of Sn and Sb at the Y site in these alloys.

In conclusion, we compare the ^{119}Sn field result in PdMnSb and Pd_2MnSb hosts with estimates of these fields available from current theoretical models. The agreement between theory and experiment is excellent for the PdMnSb host. It is proposed that the lack of as good an agreement

for the Pd_2MnSb host, on the other hand, may be a band-structure effect.

II. EXPERIMENTAL PROCEDURE

Samples of $\text{Pd}_2\text{MnSb}_{1-x}\text{Sn}_x$ ($x = 0.0075, 0.01, 0.10, 0.50, 1.0$) and $\text{PdMnSb}_{0.995}\text{Sn}_{0.005}$ were prepared by induction melting stoichiometric amounts of the desired elements using a graphite boat in a quiescent argon atmosphere. Enriched $^{119}\text{SnO}_2$ obtained from Oak Ridge National Laboratory was reduced to metallic Sn by heating to 700°C in a hydrogen atmosphere. A Mössbauer-effect spectrum of the reduced Sn samples showed no detectable trace of Sn^{4+} . 99.99% pure Pd, Mn and 99.999% pure Sn from Spex Industries Metuchen, N. J., 99.9999% pure Sb single crystal chips, and the enriched ^{119}Sn were used as starting materials. The melts were retained at 1500°C for 10 min. and 1300°C for 20 min. at which point they were quenched by passing room-temperature argon gas rapidly through the sample chamber. The ingots so obtained were powdered, sealed in evacuated ($<10^{-7}$ Torr) quartz ampules and annealed at 540°C for varying time periods. X-ray patterns of both the virgin and annealed samples were taken and revealed the $L2_1$ phase for these materials. To investigate the role of thermal history on the induction melted samples, the experimental procedure consisted of systematically recording ME spectra of the $\text{Pd}_2\text{MnSb}_{0.99}\text{Sn}_{0.01}$ samples as a function of annealing time. Since the amount of absorber material typically used (400 mg) was rather small to uniformly pack a $\frac{3}{4}$ -in. diameter lucite holder, we used MgO powder as a filler material. For heat treatment purposes the Heusler-alloy sample was physically separated from the MgO powder rather easily by cooling the mixture below 247°K and extracting the sample by a magnet. For a given heat treatment, spectra were recorded both at 300 and 78°K using a conventional

constant acceleration drive and an exchange gas cryostat. $^{119}\text{Sn}^m$ in vanadium was used as a source of the 23.8-keV γ ray for all experiments.

As an alternative method of preparation, samples of $\text{Pd}_2\text{MnSb}_{0.99}\text{Sn}_{0.01}$ and $\text{PdMnSb}_{0.995}\text{Sn}_{0.005}$ were prepared by sintering appropriate amounts of the desired elements in carefully evacuated ($<10^{-7}$ Torr) quartz ampules at 1000 and 800°C , respectively. The materials were retained at these temperatures for a 72 h period followed by a quench to room temperature and annealing at 540°C .

Samples of $\text{Pd}_{1.5}\text{MnSb}_{0.995}\text{Sn}_{0.005}$ were prepared by using $\text{Pd}_2\text{MnSb}_{0.995}\text{Sn}_{0.005}$ samples exhibiting a clear Sn magnetic field of 205 kOe, as the starting material and sintering these samples with appropriate amounts of Mn, Sb, and Sn at 900°C .

III. RESULTS

A. Annealing results on $\text{Pd}_2\text{MnSb}_{0.99}\text{Sn}_{0.01}$

Spectra of $\text{Pd}_2\text{MnSb}_{0.99}\text{Sn}_{0.01}$ and Pd_2MnSn taken at 300°K showed narrow single lines.³ This observation is consistent with the known cubic structure and Curie temperatures of Pd_2MnSb and Pd_2MnSn . On annealing the virgin samples of $\text{Pd}_2\text{MnSb}_{0.99}\text{Sn}_{0.01}$, systematic changes in both the room-temperature and liquid-nitrogen temperature spectra were observed. A least-squares fit analysis of the room temperature data to a single line is summarized in Table I. One notes that the isomer shift (IS) and size of the effect systematically increased, while the observed line-width became somewhat narrower, as a function of annealing time. On an IS plot (see Fig. 1), one observes that the general domain of the measured IS's of the $x = 0.01$ samples fall in the neighborhood of Pd_3Sn and Pd_2MnSn , and further that these IS's are significantly different from those of α -Sn, β -Sn, or SnO_2 . Pd_2MnSn , isomorphic to Pd_2MnSb ,

TABLE I. Analysis of room-temperature ^{119}Sn Mössbauer spectra of $\text{Pd}_2\text{MnSb}_{1-x}\text{Sn}_x$ samples recorded as a function of heat treatment.

$\text{Pd}_2\text{MnSb}_{1-x}\text{Sn}_x$ Sample heat treatment	Γ_{obs} (mm/sec)	IS ^a (mm/sec)	Percent absorption
$x = 0.01$ annealed 0 h	0.95(4)	-0.04(1)	3.13(8)
$x = 0.01$ annealed 12 h	0.86(2)	+0.05(1)	4.41(10)
$x = 0.01$ annealed 24 h	0.83(3)	+0.11(1)	4.18(10)
$x = 0.01$ annealed 36 h	0.89(4)	+0.10(2)	4.08(7)
$x = 0.01$ annealed ^b 84 h	0.84(4)	+0.59(10)	1.82(6)
$x = 0.10$ annealed 24 h	1.02(5)	+0.14(1)	7.2(2)
$x = 0.50$ annealed 24 h	0.89(5)	+0.11(4)	2.73(10)
$x = 1.00$ annealed 12 h	0.93(4)	+0.12(3)	8.81(8)

^a The IS are quoted relative to ^{119m}Sn in vanadium.

^b Sample annealed with MgO powder.

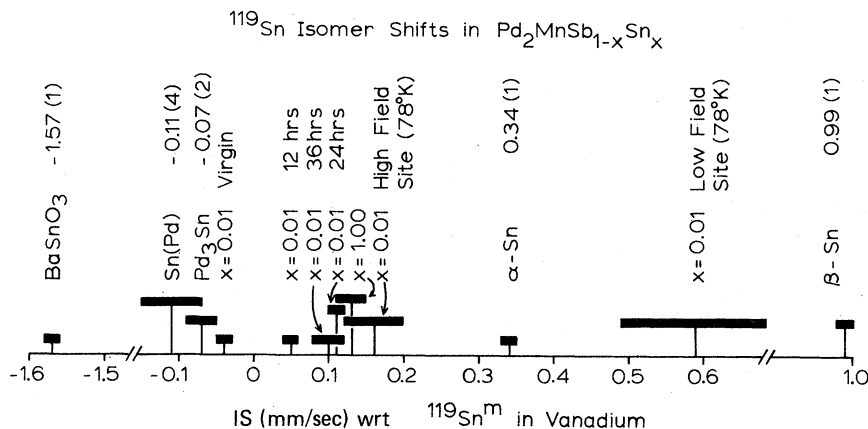


FIG. 1. Room-temperature ^{119}Sn isomer shifts of $\text{Pd}_2\text{MnSb}_{1-x}\text{Sn}_x$ samples observed as a function of heat treatment. Experimental values of the IS's appear in Table I. Low-temperature IS's of the high-field and low-field sites at $x = 0.01$ are also indicated on the line plot along with IS's of some standard Sn hosts taken from Ref. 11.

represents a case where Sn occupies the body-center position of a cubic arrangement of Pd atoms; a coordination that is anticipated for Sn if it replaces Sb in the Pd_2MnSb structure (Fig. 2). As we discuss later, we feel that these room-temperature data suggest that Sn is present in solid solution, replacing Sb in the Pd_2MnSb host.

At liquid-nitrogen temperatures ($T < T_c$), spectra of the $\text{Pd}_2\text{MnSb}_{0.99}\text{Sn}_{0.01}$ samples exhibited magnetic hyperfine splitting as expected. Spectra of the virgin samples showed evidence for two hyperfine field sites, a high-field site of 196 ± 6 kOe and an intermediate field of 101 ± 6 kOe. In Fig. 3, the smooth line fit to spectrum A represents a least squares analysis of the data to two sets of six lines, taking the g_e/g_0 ratio fixed at -0.2134 ,¹² and keeping the centroid, internal field values, and relative populations of the two sites variable. On annealing the virgin samples for a 12-h period, a noticeable change in the spectrum resulted (see spectrum B). The spectrum became more characteristic of a unique magnetic hyperfine interaction with the intensities of the outermost lines becoming larger than those of the innermost ones. The effect of annealing is to cause the population of the high-field site to increase at the expense of the intermediate field one (see Table II). On annealing the sample for a total of 24 h, the linewidth of the magnetic components reduced (see spectrum C of Fig. 3). Presumably, at this particular stage of annealing the internal field of

the high-field site becomes more unique, although here it should be indicated that the linewidths of the magnetic components (2.1 mm/sec) are still substantially larger than the linewidths encountered in the paramagnetic phase (0.83 mm/sec).

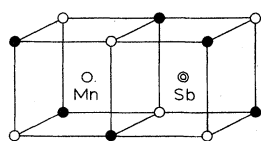


FIG. 2. Crystal structure of Pd_2MnSb ($L2_1$) and PdMnSb ($C1_b$). In the $L2_1$ structure, the open and filled circles represent Pd atoms. In the $C1_b$ structure the filled circles represent Pd atoms while the open circles Pd vacancies.

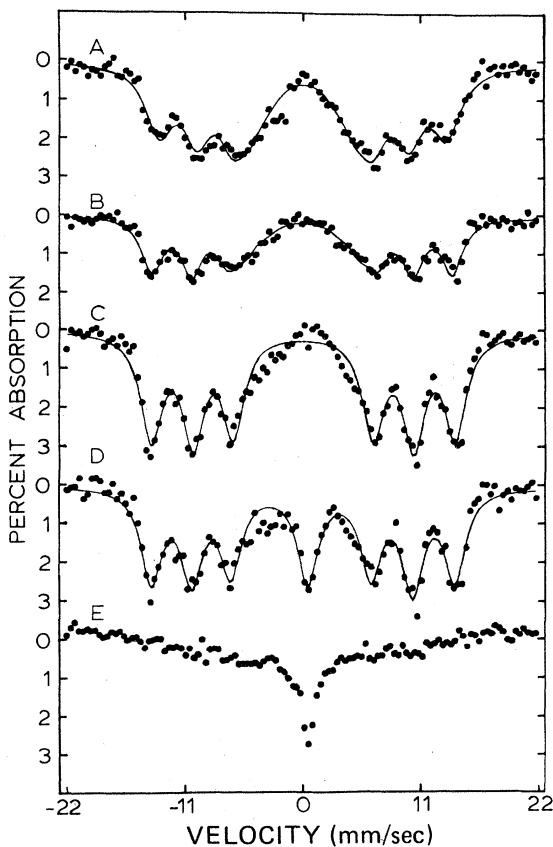


FIG. 3. ^{119}Sn Mössbauer spectra of $\text{Pd}_2\text{MnSb}_{0.99}\text{Sn}_{0.01}$ samples recorded as a function of heat treatment time t at 540°C . (A) virgin sample, $t = 0$ h; (B), $t = 12$ h; (C), $t = 24$ h; (D), $t = 36$ h; (E), $t = 84$ h. See text for other details. Table II summarizes internal field results from these spectra which were all recorded at 78°K .

TABLE II. Internal field results on $\text{Pd}_2\text{MnSb}_{1-x}\text{Sn}_x$ samples, and $\text{Pd}_{1.5}\text{MnSb}_{0.995}\text{Sn}_{0.005}$ and $\text{PdMnSb}_{0.99}\text{Sn}_{0.01}$ samples, extracted from spectra shown in Figs. 3 and 6, respectively. The subscripts h , i , and l refer to high-, intermediate-, and low-field sites.

Pd ₂ MnSb _{1-x} Sn _x Sample heat treatment	Fig. 3	Internal field					
		Magnitude (kOe)			Intensity (%)		
		H_h	H_i	H_l	I_h	I_i	I_l
$x = 0.01$ annealed 0 h	A	196(6)	101(6)	...	54	46	0
$x = 0.01$ annealed 12 h	B	205(6)	104(6)	...	77	23	0
$x = 0.01$ annealed 24 h	C	206(6)	≈100	0	0
$x = 0.01$ annealed 36 h	D	205(6)	...	<20	85	0	15
$x = 0.01$ annealed 84 h ^a	E	<20	≈100
$\text{Pd}_{1.5}\text{MnSb}_{0.995}\text{Sn}_{0.005}$ Annealed 48 h	Fig. 6	208(4)	98(8)	...	93	7	...
$\text{PdMnSb}_{0.99}\text{Sn}_{0.01}$ Annealed 12 h	Fig. 6	...	103(10)	100	...

^a Sample annealed with MgO powder.

Annealing the samples further for an additional 12 h, introduced a new feature in the spectrum, the appearance of a seventh line in the vicinity of zero velocity (see spectrum *D* of Fig. 3). The following comments are in order on this additional line, hence labeled as the third site. Its IS is +0.59(10) mm/sec, which agrees with neither metallic Sn (α or β), nor Pd_2MnSn (see Fig. 1), and further its linewidth is 2.1 mm/sec. We believe that the third site in spectrum *D* is not intrinsic to the annealing process of the HA but instead is a result of annealing the sample after stage *C* in a vacuum which was probably worse than 10^{-7} Torr. The third site can be totally avoided by sealing the samples in a vacuum better than 10^{-7} Torr. before annealing. The final piece of experimental information is contained in spectrum *E* which represents the spectrum of a sample annealed beyond stage *D* differently. In going from stage *D* to *E*, we did not physically separate the HA sample from the MgO filler material and proceeded to seal the mixture in an evacuated quartz ampule. On annealing the sample thus at 540 °C for 48 h a rather dramatic change in the ME spectrum was observed. The high-field site converted totally to the third site.

As we discuss further, we believe that the third site observed in spectra *D* and *E* results from oxygen contamination of the $\text{Pd}_2\text{MnSb}_{0.99}\text{Sn}_{0.01}$ samples. This result was checked independently by observing an enhancement of the third site at the expense of the high-field one on annealing a sample exhibiting a clear magnetic splitting (such as in spectrum *C* of Fig. 3) in a vacuum of worse than 10^{-5} Torr. Our attempts to decontaminate samples exhibiting the third site by heating to 600 °C while pumping on these with a trapped dif-

fusion pump were unsuccessful. This leads us to believe that the third site is formed irreversibly.

Spectra of $\text{Pd}_2\text{MnSb}_{0.99}\text{Sn}_{0.01}$ samples prepared by sintering the materials in a quartz tubing at 1000 °C followed by a quench to room temperature were similar to spectrum *A* in Fig. 3. On annealing these samples for a 24-h period at 600 °C, a clear magnetic hyperfine structure characteristic of the high-field site (spectrum *C* in Fig. 3) was observed.

B. ^{119}Sn fields in $\text{Pd}_2\text{MnSb}_{1-x}\text{Sn}_x$

The magnitude and sign of the Sn field in Pd_2MnSn was measured by Geldart *et al.*¹³ to be -35 ± 2 kOe. The magnitude and sign of the field at a dilute Sn impurity in Pd_2MnSb has been established by our previous work³ to be $+210 \pm 5$ kOe. In the present work we have attempted to establish the compositional behavior of the Sn field between these two extremum ($x \approx 0$, and 1) compositions. Spectra of induction melted $\text{Pd}_2\text{MnSb}_{1-x}\text{Sn}_x$ samples taken at a few compositions are reproduced in Fig. 4. These spectra are indicative of a reasonably well-defined magnetic interaction and were fit to a six-line magnetic spectrum. In Table III, a summary of the Sn fields extracted from these spectra are presented. Price *et al.*⁵ have also investigated this Heusler alloy system and the present results on the ^{119}Sn field systematics are in general agreement with their results. A point of some difference between the present data and the data of Price *et al.*⁵ can be traced to the spectrum at the composition $x = 0.10$. A spectrum of a sample taken at this composition (Fig. 4) in the present work exhibited a fairly well-defined Sn field. This spectrum does not

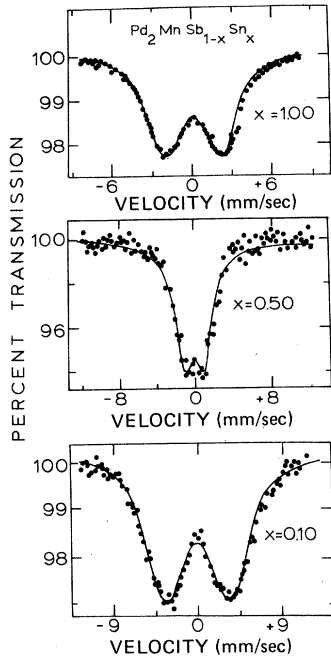


FIG. 4. ^{119}Sn Mössbauer spectra of $\text{Pd}_2\text{MnSb}_{1-x}\text{Sn}_x$ samples recorded at indicated Sn compositions x . All measurements were made at 78°K .

exhibit the nonhomogeneous field distribution seen by Price *et al.*⁵ and leads us to believe that the sample used in the present work by virtue of its preparation, could conceivably have been more homogeneous.

In Fig. 5 we have summarized the ^{119}Sn field systematics in $\text{Pd}_2\text{MnSb}_{1-x}\text{Sn}_x$ from the present work and the work of Price *et al.*⁵ Two interesting features of these field systematics are to be noted. First, there is a sharp drop in the Sn fields in the composition range $0.01 \leq x \leq 0.10$. And second, one observes a fairly continuous change in the fields from $+205$ kOe to -35 kOe between the two extreme compositions. We believe that ^{119}Sn magnetic interactions in these Heusler alloys in the composition range $0 < x \leq 0.10$ are unusually sensitive to local fluctuations in Sn concentrations in

TABLE III. Analysis of Mössbauer spectra of $\text{Pd}_2\text{MnSb}_{1-x}\text{Sn}_x$ samples recorded at 78°K (see Fig. 4). The sign of fields at $x=0.10$ and 0.50 are assigned based on systematics shown in Fig. 5.

x	Γ (mm/sec)	IS (mm/sec)	H (kOe)
0.0075	2.78(20)	+0.17(9)	+208(6)
0.01	2.23(5)	+0.18(8)	+205(5)
0.10	3.79(20)	+0.27(8)	+69(7)
0.50	2.18(8)	+0.13(4)	-14(6)
1.00	2.80(20)	+0.15(2)	-39(4)

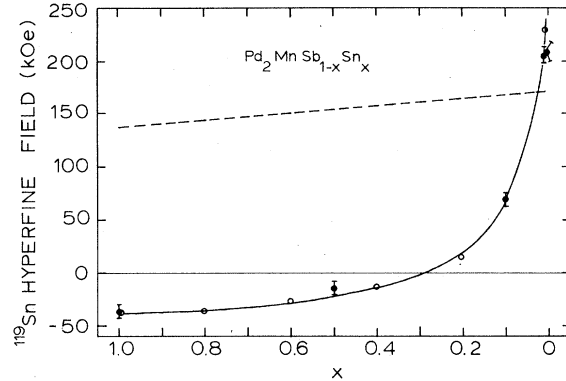


FIG. 5. ^{119}Sn fields in $\text{Pd}_2\text{MnSb}_{1-x}\text{Sn}_x$ observed as a function of Sn composition x . The filled circles represent present results, while the open circles give the results of Price *et al.* (Ref. 5). The sign of the fields at $x=0.10$ and 0.50 are assigned based on systematics. The dashed line gives the predictions of these fields based on Jena-Geldart model.

the samples because of a very strong dependence of the ^{119}Sn field on the Sn concentration in this range. The latter physical effect as we discuss further in Sec. IV B, is probably due to a band-structure effect. No attempts were made to clarify the role of sample preparation on the resulting field distribution that were observed at $x=0.02$. This represents an area that merits careful future investigations. Mössbauer spectra of $\text{Pd}_2\text{MnSb}_{1-x}\text{Sn}_x$ samples taken in the paramagnetic phase exhibited narrow single lines having IS ranging from $+0.10(2)$ to $0.14(1)$ mm/sec over the entire composition range $0 < x < 1$.

C. ^{119}Sn fields in $\text{Pd}_{1+z}\text{MnSb}_{0.995}\text{Sn}_{0.005}$

In addition to the results described in Sec. III A dealing with the composition $z=1$, we have also examined the compositions $z=0$ and $z=\frac{1}{2}$ in this Heusler alloy system and the results are as follows. Figure 6 reproduces a representative spectrum of a $z=0$ sample and the following general comments may be made. First, no significant changes in the spectra of the samples could be observed on giving these samples a variety of heat treatments, such as quenching or slow cooling the material to room temperature from 700°C , and/or prolonged annealing the material at 400°C for a week. Second, independent of the method of sample preparation, these spectra always exhibited a narrow single line near zero velocity superimposed on a broad doublet. In each case the broad doublet was fit to a six-line magnetic spectrum and yielded an average Sn field of 103 kOe at 78°K . The linewidth of the hyperfine components were typically 5.0 mm/sec

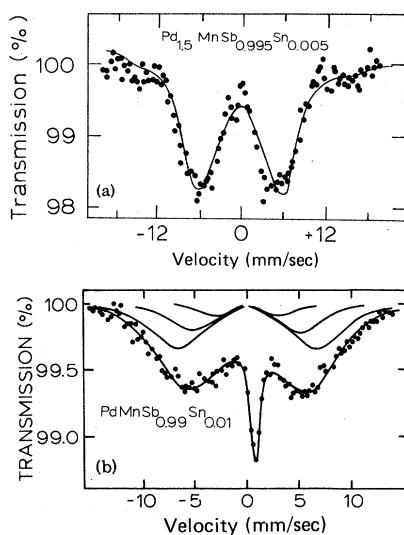


FIG. 6. ^{119}Sn Mössbauer spectra of indicated samples recorded at 78 °K.

and are thus suggestive of a broad field distribution. The IS of the magnetic component was found to be $+0.04 \pm 0.06$ mm/sec and this shift much like the IS in Pd_2MnSb is indicative of a Sn site located at the Sb site. The single line in these spectra is characterized by the following parameters: IS of $+0.74 \pm 0.03$ mm/sec and $\Gamma = 0.92 \pm 0.03$ mm/sec. This IS rules out the possibility that it represents α - or β -Sn.

Some additional confidence in the above quoted value for the Sn field in PdMnSb follows from the spectrum of $z = \frac{1}{2}$ sample in Fig. 6. The spectrum was fit to two Sn field sites keeping the high field site fixed at 208 kOe. The low-field site, which is predominant in this spectrum, gave a field value of 98 ± 8 kOe. The linewidth of the magnetic components was found to be 3.8 mm/sec. An interpretation of this data is given in Sec. IV B.

IV. DISCUSSION

A. Heat treatment effects

The present work illustrates the diverse and important metallurgical effects of Sn in the Heusler alloy system $\text{Pd}_{1+z}\text{MnSb}_{1-x}\text{Sn}_x$ that have been studied somewhat uniquely with the use of ^{119}Sn Mössbauer spectroscopy. Perhaps the most striking experimental results bear on the annealing effects observed on $\text{Pd}_2\text{MnSb}_{1-x}\text{Sn}_x$ samples. Melts of $\text{Pd}_2\text{MnSb}_{0.99}\text{Sn}_{0.01}$ when quenched to room temperature yield a defective structure. Existence of structural disorder in Pd_2MnSb host was documented by Webster¹⁴ in some of the earliest structure work on this material. We believe that by cooling the indicated melt, one quenches a large

number of Pd vacancies in the $L2_1$ structure. Sn sites having eight Pd near neighbors experience the high-field value of 210 kOe while those Sn sites having on an average four Pd near neighbors experience the intermediate field. This interpretation is suggested by the identity of the intermediate field value of 101 kOe with the Sn field in PdMnSb . Annealing $\text{Pd}_2\text{MnSb}_{0.99}\text{Sn}_{0.01}$ samples at 540 °C for 24 h promotes structural order which was in fact observed directly for the host material in x-ray diffraction patterns as a narrowing of the x-ray lines. On annealing the samples, Pd vacancies become thermally activated and annihilate with Pd interstitials. Consequently one observes in the spectra an enhancement of the high-field site at the expense of the intermediate field one. Closely similar annealing effects have been observed on the Pd_2MnSb host materials by Langouche *et al.*^{4,15} in ^{121}Sb Mössbauer spectroscopy. In these experiments, samples obtained by cooling Pd_2MnSb melts exhibited two hyperfine fields, a high-field Sb site characteristic of Pd_2MnSb and a low field one characteristic of PdMnSb . On annealing these samples the low-field site disappeared, and only the high-field site remained.⁴

Room temperature ME parameters on $\text{Pd}_2\text{MnSb}_{0.99}\text{Sn}_{0.01}$ samples obtained as a function of annealing time at 540 °C exhibit a systematic correlation with the internal field data obtained at 78 °K. Going back to the results described in Sec. III A, perhaps the most significant correlation emerges in going from the virgin samples to a sample annealed for 12 h (spectrum A to spectrum B of Fig. 3). We believe that the single-resonance line observed in the room-temperature spectra of virgin samples is really a composite of two single lines of nearly equal intensity and having slightly different IS's (<0.02 mm/sec). The single line having the more positive IS of the two lines is ascribed to Sn associated with the high-field site. The consequent reduction in observed linewidths, increase in percent absorption and more positive IS's on annealing that are documented in Table I can then be understood as resulting due to an increase in population of the high-field site at the expense of the intermediate field site.

We believe that appearance of the broad single line near zero velocity in spectra D and E of Fig. 3 results from oxygen contamination of the $\text{Pd}_2\text{MnSb}_{0.99}\text{Sn}_{0.01}$ samples on progressive annealing and that this feature is not intrinsic to Pd_2MnSb . We suggest that Sn acts as an effective trap of oxygen in a Pd_2MnSb host. Since our attempts to decontaminate such samples by heating to 600 °C in a hard vacuum were unsuccessful, we are led to believe that the Sn defect site is formed

irreversibly and is a stable entity. The only significant change observed in the spectra, following the above heat treatment to decontaminate the samples, was to narrow the linewidth of the single line from 2.1 to 1.2 mm/sec and this result then leads us to conclude that the low-field site is really a zero-field site. One can speculate on the possible structure of this "defect site" based on its IS of 0.59(10) mm/sec. This IS is larger than the IS of a Sn site substituting Sb in Pd_2MnSb and, further, it lies in the domain of the Sn IS in its divalent state as in SnO (isomer shift $\delta = +1.03$ mm/sec). Such a result could be due to the presence of oxygen in the first coordination sphere causing localization of some of the 5s and 5p-like charge density on Sn relative to the substitutional high-field Sn site.

B. Compositional effects

^{119}Sn field measurements on the $\text{Pd}_2\text{MnSb}_{1-x}\text{Sn}_x$ system reported in the present work are in general agreement with the earlier results of Price *et al.*⁵ On combining the present data with those in Ref. 5, one can clearly observe a smooth compositional variation of the ^{119}Sn field from +210 kOe at $x = 0.01$ to -35 kOe at $x = 1.00$ as shown in Fig. 5. From the room-temperature data, the measured IS's for this system are situated in a narrow range containing the IS's of Pd_2MnSn and 24-h annealed $\text{Pd}_2\text{MnSb}_{0.99}\text{Sn}_{0.01}$, both of which represent a case in which Sn has eight Pd near neighbors. This trend coupled with the smooth compositional dependence of the Sn field in $\text{Pd}_2\text{MnSb}_{1-x}\text{Sn}_x$ system, reflects in our view, the random substitution of Sn and Sb at the Y site in this Heusler alloy ($X_2\text{MnY}$) system. These observations are consistent with what is already known about the magnetic properties and crystal structure of the end-point members. Pd_2MnSb and Pd_2MnSn are known to be ferromagnetic with Curie points²² of 247 and 189 °K, and further both Heusler alloys crystallize in the cubic $L2_1$ structure with lattice parameters²² of 6.424 and 6.380 Å, respectively. Recently Webster and Ramadan²² have reported observing a smooth compositional dependence of T_c and a_0 in this system. In contrasting the compositional variation of H_{int} with that of T_c , one is struck by the similarity in behaviour and in particular by the sharp compositional dependence that occurs in the composition range $0 < x < 0.10$ for both physical parameters.

The systematics of ^{119}Sn field in $\text{Pd}_2\text{MnSb}_{1-x}\text{Sn}_x$ summarized in Fig. 5 can be broadly divided into two parts: (a) a sharply varying component in the range $0 < x < 0.10$; and (b) a slowly varying com-

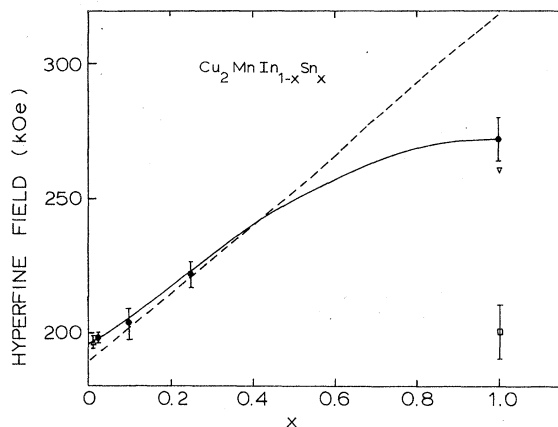


FIG. 7. ^{119}Sn fields in $\text{Cu}_2\text{MnIn}_{1-x}\text{Sn}_x$ observed (filled circles) as a function of Sn composition x . The dashed line represents calculations of these fields based on the Jena-Geldart model: \square , Geldart *et al.*, Ref. 19; \triangle Campbell *et al.*, Ref. 20; ∇ , Williams *et al.*, Ref. 21.

ponent in the range $0.10 < x < 1.0$. The reduction in Sn fields observed on replacing the pentavalent Sb by the tetravalent Sn in $\text{Pd}_2\text{MnSb}_{1-x}\text{Sn}_x$ can be understood in terms of the Jena-Geldart¹⁰ or Blandin-Campbell⁹ model, as arising due to a decrease in the induced spin polarization because of a smaller conduction-electron density (k_F). We believe that feature (b) of the ^{119}Sn field systematics is a manifestation of such an effect and can be qualitatively understood.

In Fig. 5, we project the field systematics as a function of Sn concentration x , based on the Jena-Geldart model. The lack of agreement between theory and experiment in the composition range $0.01 < x < 0.10$ is particularly significant in this case. In contrast one may indicate that a similar comparison between theory and experiment for the $\text{Cu}_2\text{MnIn}_{1-x}\text{Sn}_x$ system¹⁶ works reasonably well over the whole composition range $0 < x < 1$ (see Fig. 7). The lack of a sharp field dependence on the Sn concentration observed in the $\text{Cu}_2\text{MnIn}_{1-x}\text{Sn}_x$ system¹⁶ may be suggestive of the fact that feature (a) of the present systematics is peculiar to the presence of Pd in the present Heusler alloy system.

C. ^{119}Sn magnetic field in PdMnSb

The broad linewidths of the magnetic components for the ^{119}Sn interaction in $\text{PdMnSb}_{0.995}\text{Sn}_{0.005}$ suggest a homogeneously broadened magnetic interaction. Such a result could arise in our view, due to some degree of structural disorder around Sn, in the defect structure ($C1_b$) of PdMnSb host. To our knowledge, PdMnSn isomorphous to PdMnSb is not known to exist, and this could point towards the difficulty of substituting the Sb site in

PdMnSb by a Sn atom. On addition of Pd to $\text{Pd}_1\text{MnSb}_{1-x}\text{Sn}_x$, two significant effects occur, the solubility of Sn in the Heusler alloy phase increases (see spectrum of $z = \frac{1}{2}$ sample in Fig. 6) as the narrow single line around zero velocity in a $z = 0$ sample associated with a Sn-rich phase totally disappears. The noticeable reduction in observed linewidths of the magnetic components from 5 to 3.8 mm/sec in going from $z = 0$ to $z = \frac{1}{2}$ further suggests that the Sn-doped PdMnSb phase seems to stabilize in the presence of excess Pd. Conceivably, such a result could be due to an increase in lattice size on addition of Pd, making it more feasible for the larger sized Sn to replace Sb.

These hyperfine field data at a dilute Sn impurity in $\text{Pd}_{1+z}\text{MnSb}$ for the three compositions $z = 0, \frac{1}{2}, 1$ examined in the present work, follow a trend which is closely similar to the one reported earlier^{2,5} for the ^{121}Sb field systematics in the $\text{Pd}_{1+z}\text{MnSb}$ host. In the work of Price *et al.*⁵ ^{121}Sb spectra of $\text{Pd}_{1+z}\text{MnSb}$ samples were analyzed in terms of hyperfine field probability distributions. The results generally showed a two-peak distribution. One of the peaks was centered around 650 kOe and the other at about 300 kOe over the whole composition range $0 \leq z \leq 1$. This result was also obtained by Swartzendruber *et al.*² and shows that for a mixed composition such as $z = \frac{1}{2}$ for, e.g., Sb nuclei do not experience a unique field but instead choose two types of fields, a high field almost characteristic of Sb sites in Pd_2MnSb type of surroundings, and a low-field site nearly characteristic of Sb sites in Pd_1MnSb type of surroundings. It is therefore anticipated by analogy, that the low field observed in the present Sn experiments on $\text{Pd}_{1+z}\text{MnSb}_{0.995}\text{Sn}_{0.005}$ samples represents the field in PdMnSb. Finally, the substantially smaller solubility of Sn in PdMnSb host compared to Pd_2MnSb host, is much like the case of the Te impurity which we have recently examined in ^{125}Te and ^{129}I ME experiments.¹⁷

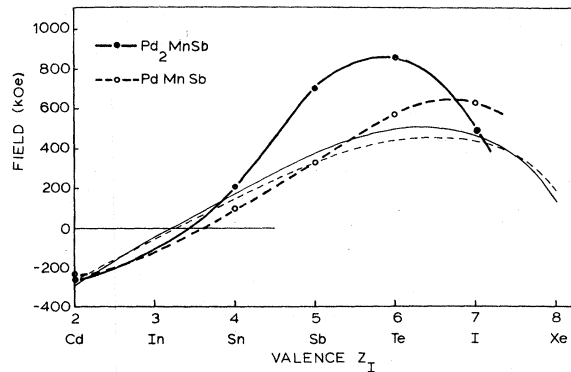


FIG. 8. Hyperfine field observed (open and filled circles) at $5sp$ elements in Pd_2MnSb and PdMnSb hosts as a function of impurity valence Z_I . The thin continuous and dashed lines are estimates of these fields based on the Jena-Geldart model.

These results are most likely the consequence of a smaller unit cell dimensions of the PdMnSb host.

D. Interpretation of ^{119}Sn fields in Pd_2MnSb and PdMnSb

The ^{119}Sn field in Pd_2MnSb and PdMnSb forms part of a general trend of fields that have been observed at other $5sp$ impurities when these substitute the Sb site in this Heusler alloy. Figure 8 summarizes these field systematics as a function of atomic valence of the sp impurity. The experimental results of the fields in PdMnSb are taken from the work of a number of investigators, and these are summarized in Table IV.

The ^{121}Sb field of 329 ± 5 kOe in PdMnSb is based on the spectrum shown in Fig. 9. In the fitting routine, the magnetic moment ratio μ_o/μ_g was taken to be 0.7486(20) from the work of Langouche *et al.*⁴ and the use of this new moment ratio probably accounts for the difference between the field quoted above and a somewhat lower field of 302 ± 5 kOe reported earlier by Swartzendruber *et al.*² The positive sign of the field derives from the work of Price *et al.*,⁵ who have observed a

TABLE IV. Summary of measured fields at $5sp$ elements in PdMnSb host. Theoretical field values in column 4 represent estimates of these fields based on the Jena-Geldart model.

$5sp$	H (kOe) Experiment	Temperature of measurement ($^{\circ}\text{k}$)	H (kOe) Theoretical	Comments
Cd	$ 255 \pm 10 $	90 ± 4	-273	Walus <i>et al.</i> , Ref. 18
In	- 80	...
Sn	$ 103 \pm 10 $	78	+126	Present work
Sb	329 ± 5	78	+330	Swartzendruber <i>et al.</i> , Ref. 2 Present work
Te	$+572 \pm 10$	4.2	+467	Boolchand <i>et al.</i> , Ref. 7
I	$ 681 \pm 6 $	4.2	+494	Boolchand, <i>et al.</i> , Ref. 17
Xe	+294	...

net increase in the Sb field on application of an external field to PdMnSb.

Price *et al.*⁵ have, in a recent review, compared various theoretical models that have been proposed to explain hyperfine fields in Heusler alloys and the reader is referred to their paper. Two models that appear to qualitatively reproduce the observed field systematics shown in Fig. 8 are due to Jena-Geldart,¹⁰ and the other is due to Blandin-Campbell.⁹ In what follows, we compare the experimental field results with the theoretical calculations of these fields based on the Jena-Geldart model. The results of these calculations for various $5sp$ impurities are summarized in Table IV. The Jena-Geldart model is an adaptation of the Daniel-Friedel model for the case of Heusler alloys. In this model one calculates the internal field H_{int} by obtaining the spin polarization $P(0)$ induced at the nonmagnetic sp impurity due to the spin-polarized conduction electrons taking into account the charge screening of the impurity. The model assumes the conduction band to be "free-electron" like and includes effects of coherent scattering, exchange and hybridization through a parameter α^2 , Bloch wave enhancement factor, that is determined from first principles for each impurity.

$$H_{\text{int}} = -\frac{1}{3}8\pi\mu_B\alpha^2P(0).$$

The existing calculations are normalized for the Sb field in PdMnSb. The excellent agreement in the magnitude of the field for the case of Sn between experiment (103 ± 10 kOe) and theory (111 kOe) is actually also reflected generally for other $5sp$ impurities where measurements are available (see Table IV). In cases where the sign of the fields have been explicitly measured, such as for Sb and Te, these calculations indeed give the correct sign. The above comparison shows that the Jena-Geldart model works rather well for the PdMnSb host.

The substantial enhancement in the Sn, Sb, and Te fields observed in going from PdMnSb host to Pd_2MnSb host are results that cannot be understood⁷ based on the Jena-Geldart model. Further the difficulty in understanding the compositional behaviour of Sn fields in the $\text{Pd}_2\text{MnSb}_{1-x}\text{Sn}_x$ system (Sec. IV B) based on this model, are indications of the limitations of this rigid-band approach. It

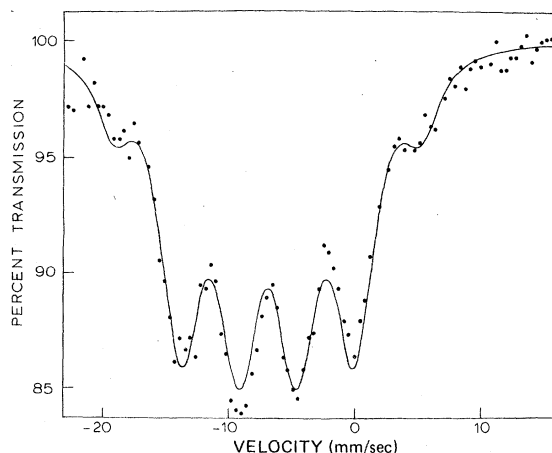


FIG. 9. ^{121}Sb Mössbauer spectrum of PdMnSb recorded at 78 °K using a Ba $^{121}\text{Sn}^{10}\text{O}_3$ source. The smooth line represents a fit of the data keeping μ_e/μ_g fixed at 0.7486(20) from Ref. 4 and yields a field of 329 ± 5 kOe. A similar fit of the data was obtained on keeping both the μ_e/μ_g and H variable and yielded best-fit values of 0.7405(75) and 322 ± 7 kOe, respectively.

appears that these internal field data on a Pd-rich Heusler alloy may be exhibiting band-structure effects arising due to the presence of a sharp d density of states of Pd at the Fermi level. A large enhancement in the density of states at the Fermi level probably occurs as one adds Pd to PdMnSb causing a significant effect on the internal field values. Elaborate band-structure calculations on Pd_2MnSb are now clearly needed to clarify the situation.

ACKNOWLEDGMENTS

We wish to acknowledge generous assistance of Bill Mitchel in the use of the induction furnace and M. Imaeda in data processing and reduction. One of us (M.T.) would like to thank the NSF for award of a Summer Undergraduate Research Fellowship. We are particularly thankful to Dr. P. Jena for clarifying theoretical aspects of the internal field calculations and in particular for making available results of the calculations indicated in this paper. This work was supported in part by the NSF and the American Philosophical Society.

*Present address: Dept. of Applied Physics, California Institute of Technology, Pasadena, Calif.

¹P. Boolchand, M. Tenhover, S. Jha, G. Langouche, B. B. Triplett, S. S. Hanna, and P. Jena, Phys. Lett. A 54, 293 (1975).

²L. J. Swartzendruber and B. J. Evans, Phys. Lett. A 38, 511 (1972).

³P. Boolchand, M. Tenhover, S. Jha, G. Langouche, B. B. Triplett, and S. S. Hanna, Solid State Commun. 21, 741 (1977).

- ⁴G. Langouche, N. S. Dixon, Y. Mahmud, B. B. Triplett, S. S. Hanna, and P. Boolchand, *Phys. Rev. C* **13**, 2589 (1976).
- ⁵D. C. Price, J. D. Rush, C. E. Johnson, M. F. Thomas, and P. J. Webster, *J. Phys. (Paris)* **37**, C6-317 (1976).
- ⁶H. deWaard, F. th ten Broek, and N. Teekens, in *Hyperfine Interactions IV*, edited by R. S. Raghavan and D. E. Murnick (North-Holland, Amsterdam, 1978), p. 381.
- ⁷P. Boolchand, M. Tenhover, M. Marcuso, M. Blizzard, C. S. Kim, G. Langouche, M. Van Rossum, and R. Coussement, in *Hyperfine Interactions IV*, edited by R. S. Raghavan and D. E. Murnick (North-Holland, Amsterdam, 1978), p. 388.
- ⁸C. C. M. Campbell and W. Leiper, in Conference on Magnetism and Magnetic Materials, Boston, 1973, p. 319 (unpublished); *C. C. M. Campbell, J. Phys. F* **5**, 1931 (1975).
- ⁹A. Blandin and I. A. Campbell, *Phys. Rev. Lett.* **31**, 51 (1973).
- ¹⁰P. Jena and D. J. W. Geldart, *Solid State Commun.* **15**, 139 (1974).
- ¹¹*Mössbauer Effect Data Index* (covering 1972 literature), edited by J. Stevens and V. Stevens (Plenum, New York, 1973), p. 277.
- ¹²The value of $g_e/g_0 = -0.2134$ is taken from an average of number of measurements summarized by N. N. Greenwood and T. C. Gibbs, in *Mössbauer Spectroscopy* (Chapman and Hall, London, 1971), p. 380.
- ¹³D. J. W. Geldart, C. C. M. Campbell, P. J. Pothier, and W. Leiper, *Can. J. Phys.* **50**, 206 (1972).
- ¹⁴P. J. Webster and R. S. Tebble, *J. Appl. Phys.* **39**, 471 (1968); *Philos. Mag.* **16**, 347 (1967).
- ¹⁵G. Langouche (private communication of unpublished results).
- ¹⁶M. Tenhover and P. Boolchand (unpublished).
- ¹⁷P. Boolchand, M. Tenhover, and P. Jena, *Phys. Rev. B* (to be published).
- ¹⁸W. Walus, R. Goss-Zurek, B. Styczen, C. Szytuta, and J. Styczen, in *Proceedings of International Conference on Hyperfine Interactions Studied in Nuclear Reactions and Decay, Uppsala, 1974*, p. 182 (unpublished).
- ¹⁹D. J. W. Geldart, C. C. M. Campbell, P. J. Pothier, and W. Leiper, *Can. J. Phys.* **50**, 206 (1972).
- ²⁰C. C. M. Campbell, *J. Phys. F* **5**, 1931 (1975).
- ²¹J. M. Williams, *J. Phys. Colloq. Suppl.* **32**, C1, 790 (1971).
- ²²P. J. Webster and M. R. I. Ramadan, *J. Magn. Mater.* **5**, 57 (1977).